

Dartmouth College

Dartmouth Digital Commons

Open Dartmouth: Published works by
Dartmouth faculty

Faculty Work

11-13-2017

Small RNA teg49 Is Derived from a sarA Transcript and Regulates Virulence Genes Independent of SarA in Staphylococcus aureus

Adhar Manna

Dartmouth College, Adhar.C.Manna@Dartmouth.edu

Samin Kim

Dartmouth College

Liviu Cengher

Dartmouth College

Anna Corvaglia

Geneva University Hospital

Stefano Leo

Geneva University Hospital

See next page for additional authors

Follow this and additional works at: <https://digitalcommons.dartmouth.edu/facoa>



Part of the [Medical Genetics Commons](#), and the [Medical Immunology Commons](#)

Dartmouth Digital Commons Citation

Manna, Adhar; Kim, Samin; Cengher, Liviu; Corvaglia, Anna; Leo, Stefano; Francois, Patrice; and Cheung, Ambrose L., "Small RNA teg49 Is Derived from a sarA Transcript and Regulates Virulence Genes Independent of SarA in Staphylococcus aureus" (2017). *Open Dartmouth: Published works by Dartmouth faculty*. 932.

<https://digitalcommons.dartmouth.edu/facoa/932>

This Article is brought to you for free and open access by the Faculty Work at Dartmouth Digital Commons. It has been accepted for inclusion in Open Dartmouth: Published works by Dartmouth faculty by an authorized administrator of Dartmouth Digital Commons. For more information, please contact dartmouthdigitalcommons@groups.dartmouth.edu.

Authors

Adhar Manna, Samin Kim, Liviu Cengher, Anna Corvaglia, Stefano Leo, Patrice Francois, and Ambrose L. Cheung



Small RNA teg49 Is Derived from a *sarA* Transcript and Regulates Virulence Genes Independent of SarA in *Staphylococcus aureus*

Adhar C. Manna,^{a,b} Samin Kim,^{a*} Liviu Cengher,^a Anna Corvaglia,^c Stefano Leo,^c Patrice Francois,^c Ambrose L. Cheung^a

^aDepartment of Microbiology and Immunology, Geisel School of Medicine at Dartmouth, Hanover, New Hampshire, USA

^bDepartment of Biological Sciences, Presidency University, Kolkata, India

^cGenomic Research Laboratory, Services of Infectious Diseases, Geneva University Hospital, Geneva, Switzerland

ABSTRACT Expression of virulence factors in *Staphylococcus aureus* is regulated by a wide range of transcriptional regulators, including proteins and small RNAs (sRNAs), at the level of transcription and/or translation. The *sarA* locus consists of three overlapping transcripts generated from three distinct promoters, all containing the *sarA* open reading frame (ORF). The 5' untranslated regions (UTRs) of these transcripts contain three separate regions ~711, 409, and 146 nucleotides (nt) upstream of the *sarA* translation start, the functions of which remain unknown. Recent transcriptome-sequencing (RNA-Seq) analysis and subsequent characterization indicated that two sRNAs, teg49 and teg48, are processed and likely produced from the *sarA* P3 and *sarA* P1 transcripts of the *sarA* locus, respectively. In this report, we utilized a variety of *sarA* promoter mutants and *csH*A and *rnc* mutants to ascertain the contributions of these factors to the generation of teg49. We also defined the transcriptional regulon of teg49, including virulence genes not regulated by SarA. Phenotypically, teg49 did not impact biofilm formation or affect overall SarA expression significantly. Comparative analyses of RNA-Seq data between the wild-type, teg49 mutant, and *sarA* mutant strains indicated that ~133 genes are significantly upregulated while 97 are downregulated in a teg49 deletion mutant in a *sarA*-independent manner. An abscess model of skin infection indicated that the teg49 mutant exhibited a reduced bacterial load compared to the wild-type *S. aureus*. Overall, these results suggest that teg49 sRNA has a regulatory role in target gene regulation independent of SarA. The exact mechanism of this regulation is yet to be dissected.

KEYWORDS RNA-Seq, *S. aureus*, SarA, biofilms, gene expression, gene regulation, mouse model, small RNAs

Staphylococcus aureus is both a commensal and an opportunistic pathogen that causes a broad range of human and animal infections. The diseases can range from acute food poisoning, pneumonia, meningitis, superficial skin infections (e.g., acne, boils, or cellulitis), arthritis, osteomyelitis, or endocarditis to toxic shock syndrome (1, 2). Besides demonstrating a capacity to rapidly develop resistance to many antibiotics, including vancomycin, *S. aureus* has an ability to thwart the innate host defense systems, included those provided by neutrophils and macrophages (3, 4). In addition, staphylococcal infections are common after viral infections. Not surprisingly, *S. aureus* infections are frequently associated with high mortality, morbidity, and health-related costs.

The pathogenesis of *S. aureus* is a complex process that involves multiple virulence

Received 2 September 2017 Returned for modification 9 October 2017 Accepted 30 October 2017

Accepted manuscript posted online 13 November 2017

Citation Manna AC, Kim S, Cengher L, Corvaglia A, Leo S, Francois P, Cheung AL. 2018. Small RNA teg49 is derived from a *sarA* transcript and regulates virulence genes independent of SarA in *Staphylococcus aureus*. *Infect Immun* 86:e00635-17. <https://doi.org/10.1128/AI.00635-17>.

Editor Nancy E. Freitag, University of Illinois at Chicago

Copyright © 2018 American Society for Microbiology. All Rights Reserved.

Address correspondence to Adhar C. Manna, Adhar.C.Manna@Dartmouth.edu, or Patrice Francois, patrice.francois@genomic.ch.

* Present address: Samin Kim, Yongsan International School of Seoul, Seoul, South Korea.

A.C.M. and S.K. contributed equally to this work.

factors, specifically, surface proteins, invasive enzymes and proteases, immunological disguises, membrane-damaging toxins, exotoxins, and inherent and acquired resistance to antimicrobial agents (1, 5). The expression of many virulence factors is primarily controlled by global regulatory systems, including two-component regulatory systems (TCS) (e.g., *agr*, *lytSR*, and *saeRS*) and transcriptional regulators (e.g., at least 10 SarA family proteins, *tcaR*, and *sigB*) (6–9). Among these, the best characterized are the *agr* locus, which represents a prototypic two-component quorum-sensing system (10, 11), and the *sarA* locus (12), which can regulate directly and indirectly a large number of genes involved in virulence, autolysis, biofilm formation, stress responses, antibiotic resistance, and metabolic processes (6, 8, 13–15).

The *sarA* locus is a complex regulatory system comprising three promoters (P2, P3, and P1) that yield three distinct but overlapping transcripts (*sarA* P2, *sarA* P3, and *sarA* P1), each containing the *sarA* open reading frame (ORF) (16). The expression of these transcripts is known to be growth phase dependent, with the P2 and P1 promoters being σ^A dependent and the σ^B -dependent P3 promoter expressed during the post-exponential phase of growth (16, 17). Although the expression of the three transcripts varies with the growth phase, the overall level of SarA production remains relatively constant until the cell culture reaches the stationary phase of growth, when SarA expression appears to be higher, presumably as the summation of SarA translation from the combined *sarA* transcripts (18, 19). The complexity of *sarA* regulation is due in part to the presence of an unusually long (~850-bp) region upstream of the *sarA* coding sequence that is required for optimal expression of SarA and its target genes throughout the growth cycle (20).

Recently, it was shown that a number of small RNAs (sRNAs) are involved in the regulation of virulence genes in various organisms, including *S. aureus* (21–24). Small RNAs are classified based on their target regulation: *cis*-acting sRNAs, such as in binding to the complementary mRNA (antisense), or *trans*-acting, such as those that bind target RNA or proteins at distal sites (21). There are at least 303 potential sRNAs in various *S. aureus* genomes, only 92 of which have been positively confirmed by independent experimental methods (24, 25). The most studied sRNA in *S. aureus* is *agr* RNAIII, which is the effector of the *agr* system through competitive binding to mRNA of the target genes (26), including *mgrA*, *hla*, and *spa* mRNAs (22, 27). There are several well-characterized sRNAs, including *rsaE*, which coordinates the downregulation of *oppB* and *opp-3A* (amino acid and peptide transporter) and *sucC* (succinyl-coenzyme A synthase) mRNAs to inhibit translation (28); *artR*, which is involved in activating alpha toxin expression by targeting the 5' untranslated region (UTR) of *sarT* mRNA (29); and *sprD*, which represses the translation of *sbi* mRNA (an immunoglobulin binding protein) (30). Another unique sRNA is the dual-function PSM-*mec* gene, which confers methicillin resistance through the cytolytic toxin PSM α and inhibits the translation of *agrA* mRNA through 5'-end base pairing (31). Transcriptome-sequencing (RNA-Seq) analysis of the *sarA* locus disclosed two sRNAs, teg49 and teg48, with teg49 residing within the *sarA* P3 and P1 promoter region and involved in virulence gene expression (25, 32).

In this study, we constructed various *sarA* promoter and *csH*A and *rnc* (RNase III) mutant strains to understand the mechanism of teg49 generation in *S. aureus*. We also evaluated the transcriptome of the teg49 mutant, showing both SarA-dependent and SarA-independent gene regulation. These results indicated that the overall expression of SarA and biofilm formation were not significantly altered due to deletion of the teg49 region. RNA-Seq analyses of the teg49 mutant compared to wild-type (wt) and *sarA* mutant strains indicated that about 133 upregulated genes and 97 downregulated genes are specifically regulated by teg49. RNA-Seq data also revealed that 10 putative regulatory (e.g., *saeRS* and *rbsU*) and 34 putative virulence (e.g., *sbi*, *map*, *lukSF*, *coa*, *setnM*, and *smc*) genes are regulated by teg49, in addition to a large number of metabolic genes and genes with unknown functions. Validation of potential teg49-regulated genes by quantitative real-time PCR (qRT-PCR) confirmed the validity of the alteration of gene expression. The *in vivo* significance of the teg49 mutant, along with the hairpin loop 1 (HP1) mutant, of teg49 was assessed using the murine model of skin

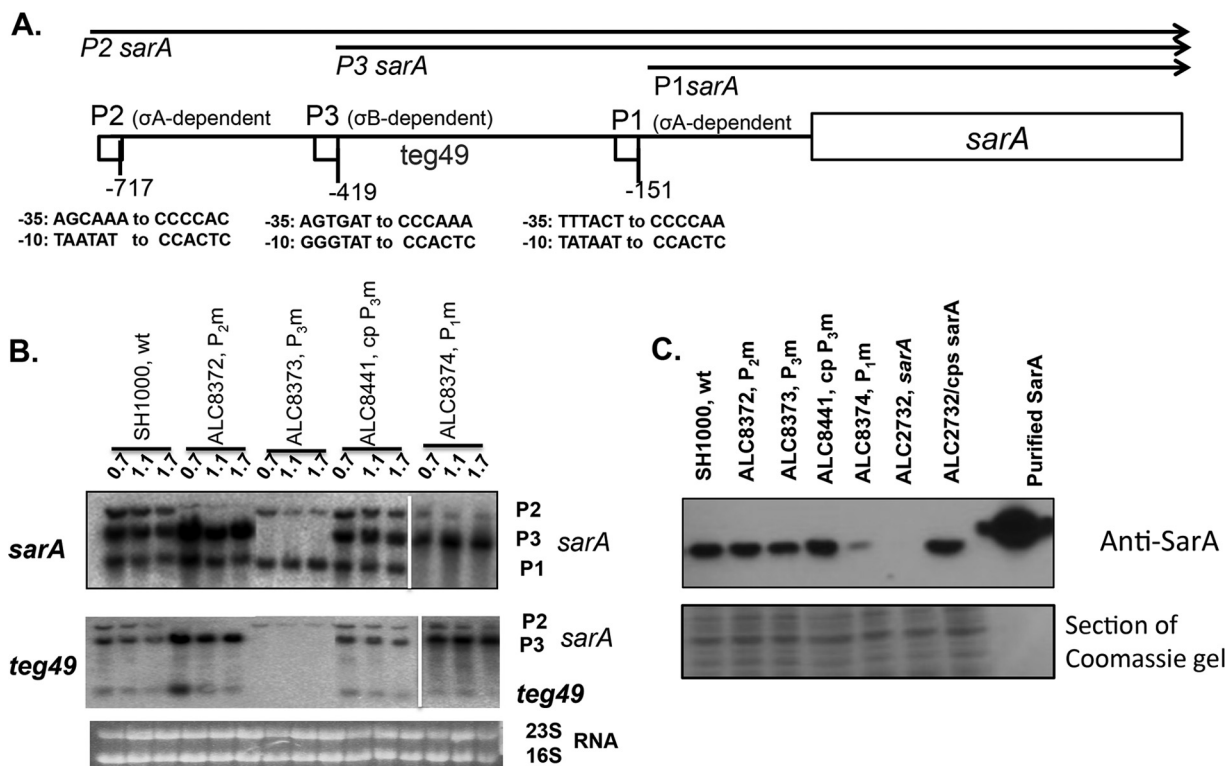


FIG 1 Expression of the *sarA* transcripts and *teg49* sRNA from *sarA* promoter mutants at various phases of growth in *S. aureus*. (A) Schematic representation of the *sarA* locus showing various transcripts (*sarA* P₂, *sarA* P₃, and *sarA* P₁) that originate from the P₂, P₃, and P₁ promoters (arrows), respectively. The *sarA* open reading frame is indicated by a box, and the promoters are indicated by small boxes. The numbers of the promoter locations are based on the start codon (ATG) of the *sarA* gene. (B) Northern blot analysis of total RNA isolated from the wild-type SH1000 and the various isogenic promoter mutants at various phases of growth recorded as OD₆₀₀ values (OD₆₀₀ values of 0.7, 1.1, and 1.5 represent mid-log, late log, and early stationary phases, respectively). In all the gels, 10 μg of total cellular RNA was loaded onto each lane, and the blots were probed with a 375-bp *sarA* DNA probe containing the *sarA* ORF (top) or a 180-bp DNA fragment containing *teg49* (middle). The 16S and 23S rRNAs of the ethidium bromide-stained gel used for blotting is also shown as a loading control at the bottom. The spliced images were taken from different regions of the same image. (C) Western blot analysis for SarA, with anti-SarA antibody, of the wild type, its isogenic promoter mutants, the *sarA* mutant, and a complemented mutant. Equivalent amounts of extracts (10 μg) from the late exponential phase of growth (OD₆₀₀ ≈ 1.1) were used to detect SarA protein. (Bottom) A Coomassie blue-stained duplicate-run gel used for blotting is shown as a loading control.

abscess infection; the results indicated that the *teg49* mutant showed a reduced bacterial load in infected skin tissues versus the parental strain. Overall, these results suggest that *teg49* sRNA has a regulatory role in target virulence gene regulation in *S. aureus*, although the exact mechanism of its action has yet to be dissected in detail.

RESULTS

Analysis of factors involved in the generation of *teg49* sRNA. In prior studies, Beaume et al. (25) identified, by RNA-Seq of strain N315, two sRNAs, *teg49* and *teg48*, within the *sarA* locus. In subsequent studies, we demonstrated the existence of *teg49* and *teg48* sRNAs within the *sarA* locus by Northern blotting and primer extension studies in strain Newman (32). The *teg49* sRNA, located within the *sarA* P₃-P₁ promoter region (Fig. 1A), is 196 nucleotides (nt) in length. To determine precisely the origin of the *teg49* sRNA, we first constructed various *sarA* promoter mutants in the SH1000 background. Accordingly, the -35 and -10 promoter sequences of all three *sarA* transcripts, P₂, P₃, and P₁, were altered by site-directed mutagenesis, as shown in Fig. 1A. Promoter-specific knockout mutants were then constructed, utilizing the temperature-sensitive origin-of-replication shuttle vector pMAD, and verified by PCR, DNA sequencing, and Northern analysis, as described in Materials and Methods. To verify the mutation, we ascertained that the corresponding P₂, P₃, or P₁ transcript was absent or markedly reduced in the respective promoter mutants (ALC8372 [P₂m], ALC8373 [P₃m], and ALC8374 [P₁m] mutants) when probed with a fragment containing the *sarA* ORF

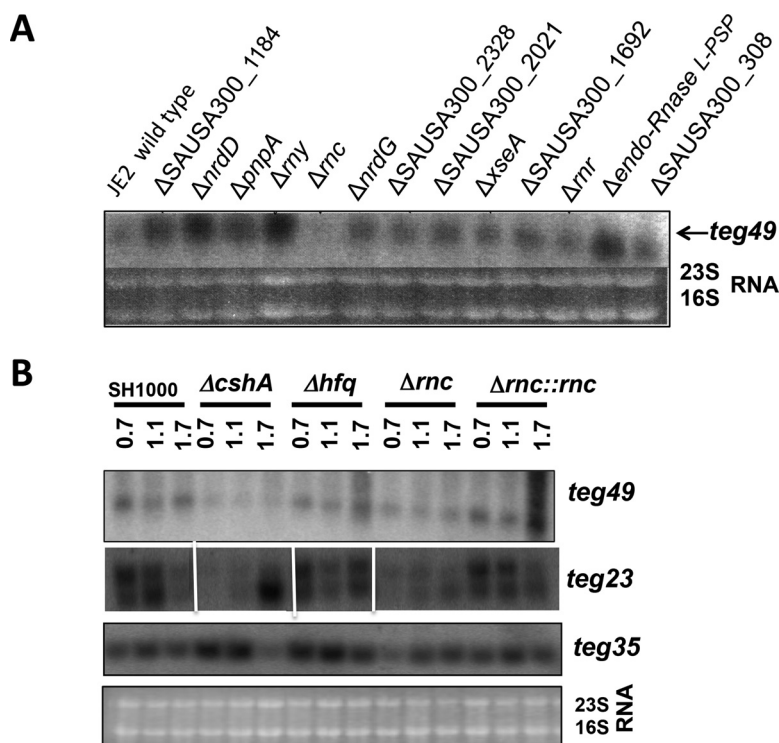


FIG 2 Northern blots of diverse mutants to determine the expression of teg49 and teg23 sRNAs. (A) Northern blot analysis for the teg49 sRNA in the wild-type JE2 and its isogenic RNase and other putative mutants as indicated. (B) Northern blot analyses to determine the expression of sRNAs (teg49, teg23, and teg35) in the wild-type, *cshA*, *hfq*, *rnc*, and complemented *rnc* strains hybridized with radiolabeled 180-bp teg49, 190-bp teg23, and 225-bp teg35 probes. A total of 10 μ g of cellular RNA from the various phases of growth was loaded onto each lane. An ethidium bromide-stained gel used for blotting, showing 16S and 23S rRNA bands, is shown as the loading control. The spliced images are taken from different regions of the same image. The numbers above the gels are OD₆₀₀ values.

(Fig. 1B, top). These mutants were then analyzed for expression of the teg49 sRNA. Importantly, a band corresponding to the teg49 sRNA was absent in ALC8373 (the P3 promoter mutant) but was present in ALC8372 (the P2 promoter mutant) and ALC8374 (the P1 promoter mutant), while the restored P3 promoter strain (ALC8441) was able to reestablish both the P3 *sarA* mRNA and the teg49 sRNA (Fig. 1B, bottom). These data indicate that the teg49 transcript likely originates from the P3 *sarA* mRNA, presumably via specific cleavage.

The lack of teg49 in the *sarA* P3 promoter mutant suggests that the *sarA* P3 transcript may be processed to yield teg49, a stable sRNA species that can be detected by Northern, primer extension, and real-time PCR (RT-PCR) analyses (32). One possibility is that this processing step may involve a specific endoribonuclease(s). To verify this possibility, we examined the expression of the teg49 sRNA in putative RNase mutants in the *S. aureus* JE2 library from the University of Nebraska (33). As shown in Fig. 2A, only the RNase III (*rnc*) mutant of JE2 failed to express teg49 among these putative RNase mutants, while an elevated level of expression was observed in Δ nrdD (anaerobic ribonucleotide reductase large subunit; SauUSA300_2551), Δ my (RNaseY; SAOUHSC_01179), and Δ endo-RNase L-PSP (putative endoribonuclease L-PSP; SauUSA300_0474) mutants. There were no significant reductions in the levels of teg49 in nine other mutants, i.e., Δ SauUSA300_1184 (a conserved hypothetical protein similar to thiamine binding protein), Δ pnpA (polyribonucleotidyltransferase; SauUSA300_1167), Δ nrdG (anaerobic ribonucleotide reductase small subunit; SauUSA300_2550), Δ SauUSA300_2328 (conserved hypothetical protein), Δ SauUSA300_2021 (S1 RNA binding domain protein Tex), Δ xseA (exodeoxyribonuclease VII large subunit; SauUSA300_1472), Δ SauUSA300_1692 (conserved hypothetical protein), Δ rrn (RNase R, SauUSA300_0764) mutants and a

control Δ SauUSA300_0308 (putative ABC transporter; permease) mutant. For confirmation, we constructed an *rnc* deletion mutant, as well as a *trans*-complemented mutant, in the SH1000 background. As can be seen in Fig. 2B (top), the expression of *teg49* was markedly diminished in the *rnc* mutants and was restored to nearly parental level in the complemented mutant (ALC8445).

In an earlier study, we showed that CshA, a DEAD box RNA helicase, protects *sarA* mRNAs from the endoribonuclease cleavage of the *mazF* toxin in strain Newman (34). Contrary to the usual role of CshA as part of the degradosome to degrade mRNA, CshA has been linked to the expression and stability of *teg49* and possibly 21 other sRNAs (out of 85 sRNAs examined), as detected by NanoString analysis in strain Newman (34). To confirm this finding in SH1000, we verified by Northern analysis that expression of *teg49*, and also *teg23*, another sRNA protected by CshA, was diminished in the *cshA* mutant versus the parent while expression of *teg35*, the control sRNA not affected by CshA (34), was found to be elevated in the *cshA* mutant versus the parent, as one would predict if *teg35* is processed as part of the degradosome (Fig. 2B, bottom). Hfq, a chaperone that binds and stabilizes many sRNAs in Gram-negative species, did not have any major impact on the expression of *teg49*, *teg23*, and the control sRNA, *teg35* (Fig. 2B). Notably, the expression of *teg23* was also diminished in the Δ *rnc* mutant of SH1000 and was restored to the parental level in the complemented mutant, while *rnc* had no effect on the expression of *teg35*.

Effect of the *sarA* P3 promoter on SarA expression. The generation of *teg49* from the *sarA* P3 transcript implied that a P3 promoter mutant would have a dual effect on reducing expression of *sarA* P3 mRNA and *teg49*. In our previous studies (32), our data seemed to suggest that *teg49* may have regulatory activity on its own independent of *sarA*. To assess the dual effect of *sarA* P3 mRNA and *teg49* in the P3 promoter mutant on SarA protein expression, immunoblots of whole-cell lysates of various promoter mutants, along with the wild-type and P₃m revertant strains, were probed with monoclonal anti-SarA antibody. As shown in Fig. 1C, the P₃m promoter mutant (ALC8373) exhibited a moderate reduction in SarA expression of 30% \pm 15% at an optical density at 600 nm (OD₆₀₀) of \sim 1.1 compared to the wild type (set at 100% by ImageJ analysis), while the SarA protein level was restored in the revertant mutant (ALC8441). As a comparison, there was no significant decrease in the SarA protein level for the P₂m promoter mutant (ALC8372) compared to the wild-type strain. However, a significant decrease in the SarA protein level was observed in the P₁m promoter mutant (ALC8374), with a reduction of 75% \pm 15% at an OD₆₀₀ of \sim 1.1 with respect to the wild-type strain (100%). As a control, the *sarA* deletion mutant did not exhibit any SarA protein expression, but this defect was restored to the parental level upon complementation (ALC2732). Together, these data revealed a moderate decrease in the SarA protein level in a P₃ promoter mutant in which the *sarA* P3 mRNA and *teg49* are absent. Given that the *sarA* P1 promoter mutant can express *teg49* at a normal level (Fig. 1B), accompanied by significantly reduced SarA expression (Fig. 1C), it is unlikely that SarA is involved in the production of *teg49*.

Effects of *teg49* on the *sarA* P3 transcript and SarA expression. Given our finding on the SarA protein level in the *sarA* P3 promoter mutant, we wanted to dissect the role of *teg49* in SarA expression. Accordingly, we constructed a 204-bp deletion mutant of *teg49* (ALC7907) (Fig. 3A) and a *trans*-complemented mutant (ALC7912) by introducing a xylose-inducible promoter vector, pEPSA5, driving a 196-bp *teg49* fragment (32). While the P1 *sarA* mRNA can be detected in assorted strains of the *teg49* mutant, the P3 mRNA is noticeably absent in the *teg49* mutants (ALC7907 and ALC7910) (Fig. 3B). To rule out the possibility that deletion of *teg49* may disrupt the *sarA* P3 transcript, we *trans*-complemented the Δ *teg49* strain with the pEPSA5 plasmid driving the expression of *teg49* (ALC7912). As shown in Fig. 3B, this strain expressed both the *sarA* P1 transcript (591 nt long) and a truncated P3 *sarA* transcript (\sim 650 nt long) due to the chromosomal *teg49* deletion. This result indicated that deletion of *teg49* affects the expression of the *sarA* P3 transcript and that overexpression of *teg49* may help stabilize

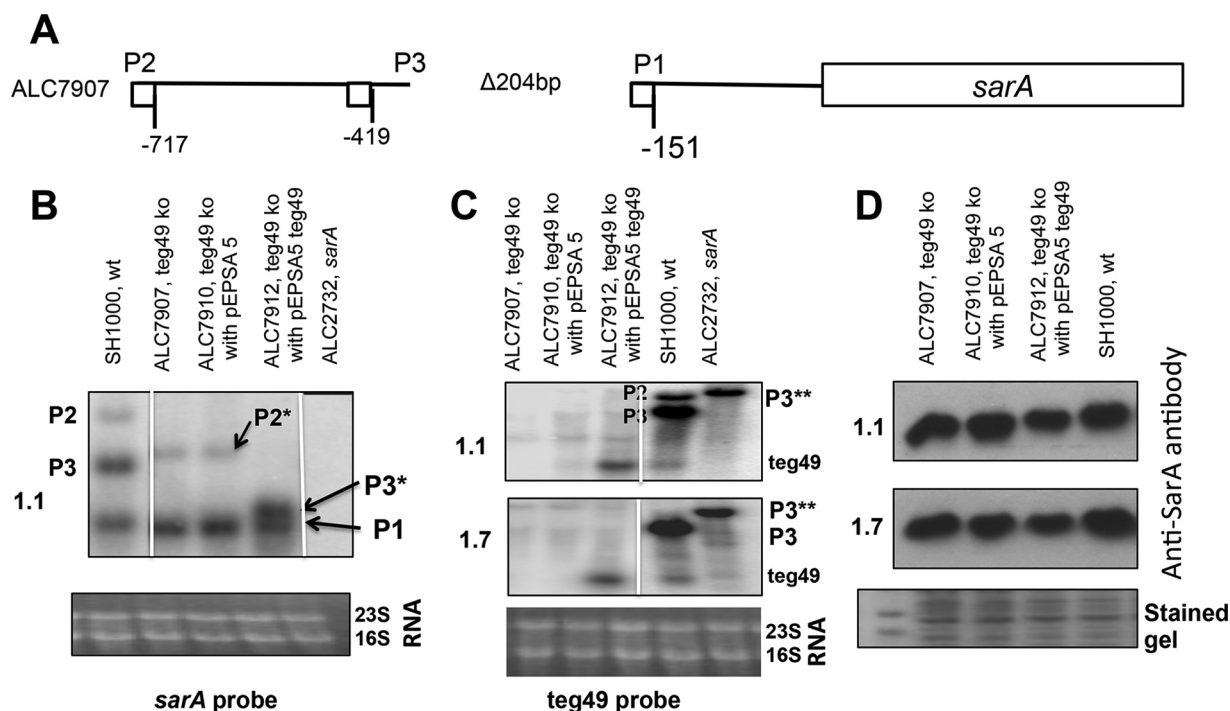


FIG 3 Expression of *sarA* transcripts and *teg49* sRNA in the *teg49* mutant and its derivative strains at various phases of growth in *S. aureus*. (A) Schematic representation of the *teg49* mutant showing the region deleted to construct the mutant (ALC7907). (B and C) Northern analysis of RNA isolated from the wild-type SH1000, *teg49* mutant (7907), *teg49* mutant with pEPSA5 (7910), and *teg49* mutant with pEPSA5::*teg49* and the *sarA* deletion mutant (ALC2732) at different growth phases. The blots were probed with a 375-bp DNA probe containing the open reading frame of the *sarA* gene (B) or a 180-bp DNA fragment containing *teg49* (C). The 16S and 23S rRNA bands in an ethidium bromide-stained gel served as loading controls. Various *sarA* transcripts (P2, P3, and P1) are marked, while P2* and P3* (B) indicate the corresponding truncated transcripts due to deletion of the *teg49* region. P3** (C) denotes the size of the P3 transcript in the *sarA* mutant of SH1000, where the *sarA* gene has been replaced by *ermC*. The spliced images were taken from different regions of the same image. (D) Western blot analyses for SarA with anti-SarA antibody of the wild type, the *teg49* strain, and its isogenic derivative strains from panels B and C. Equivalent amounts of extracts (10 μg) from the different phases of growth ($\text{OD}_{600} \approx 1.1$, late exponential phase; $\text{OD}_{600} \approx 1.7$, postexponential phase) were used to detect SarA protein. (Bottom) A section of Coomassie blue-stained duplicate-run gel used for blotting is shown as a loading control for all the gels. All the strains containing pEPSA5 and its derivatives were grown in the presence of 2% xylose to induce *teg49* expression. The numbers at the left of the gels are the OD_{600} values.

the P3 *sarA* transcript in a *teg49* mutant strain; alternatively, *teg49* may somehow affect *sarA* P3 promoter activity. As expected, the *teg49* transcript was detected in the *trans*-complemented *teg49* strain (ALC7912), but not in the Δteg49 mutant strain (Fig. 3C). To ascertain if deletion of *teg49* would alter SarA protein expression independently of the *sarA* P3 promoter activity, we performed Western blot analysis of the whole-cell lysate from ALC7907 (Δteg49) and its derivative strains containing pEPSA5 (vector; ALC7910) or the complemented plasmid, pEPSA5::*teg49* (ALC7912), along with the wild type, using monoclonal anti-SarA antibody 1F1. As shown in Fig. 3D, the changes in the SarA protein level for these strains in two growth phases were not significant ($15\% \pm 10\%$), as measured by densitometric scanning with ImageJ. Overall, these results support the notion that the *sarA* P3 transcript contributed moderately to the expression of SarA inside the cell and that *teg49* contained within the *sarA* P3 transcript is not a major contributor to SarA expression.

Biofilm formation and expression of some virulence genes in the *teg49* mutant. Several studies have disclosed the critical role of SarA in regulation of biofilm formation in *Staphylococcus* species (13, 35). To determine the role of the *teg49* mutant in biofilm formation, biofilm assays were performed (Fig. 4A). Concordant with a lack of effect on the SarA protein level, the *teg49* mutant exhibited biofilm formation similar to that of the parental strain, SH1000, and the complemented mutant. Expression of biofilm-related genes, such as the *icaRA* genes, was also found not to be affected by inactivation or overexpression of *teg49* (Fig. 4B). Collectively, these data indicate that *teg49* is not a major contributor to biofilm formation in strain SH1000.

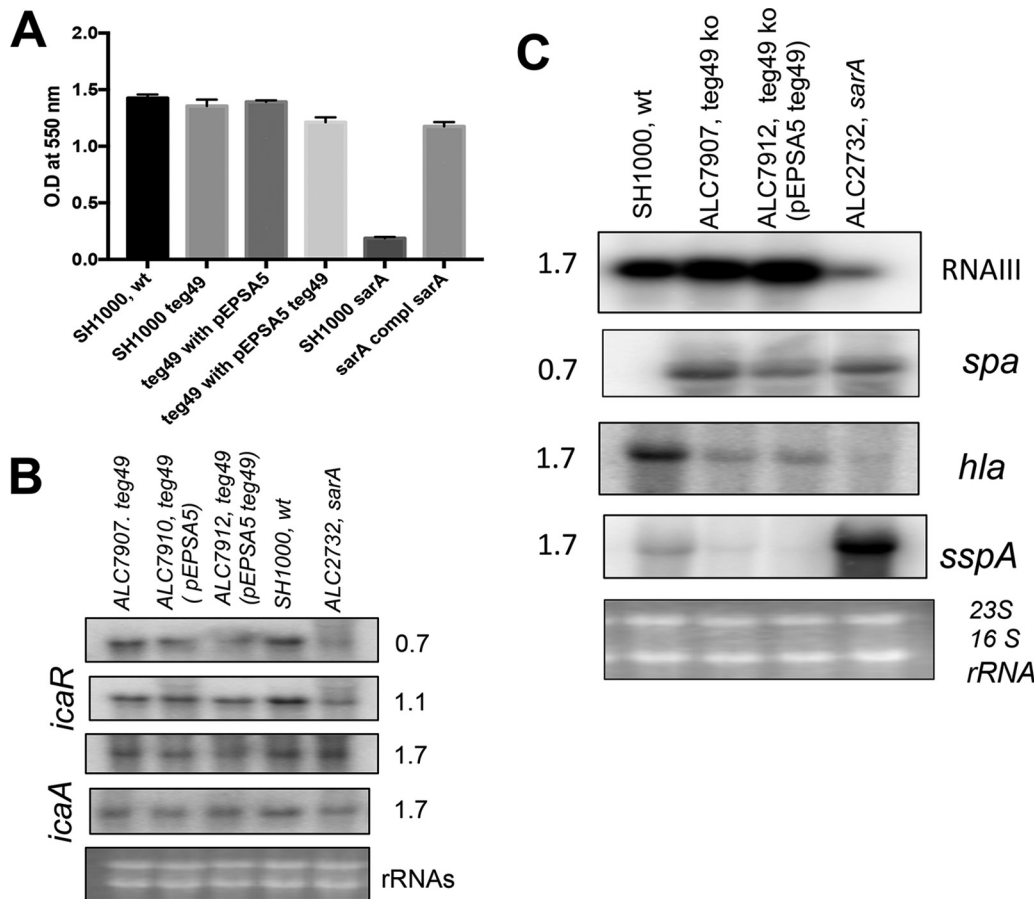


FIG 4 Phenotypic and genetic analyses for biofilm formation and selective virulence gene expression for the *teg49* mutant and its derivative strains. (A) Biofilm formation by various strains in microtiter wells containing TSB and 0.25% glucose. The cells were grown for 24 h, and the biofilms were stained with crystal violet and solubilized with acetic acid to read OD₅₅₀. The *sarA* mutant and complemented mutant were used as negative and positive controls, respectively. The results are expressed as means and standard errors of the mean. (B) Northern blots for the wild-type, *teg49* mutant, *teg49* containing pEPSA5, *teg49* mutant containing pEPSA5::*teg49*, and isogenic *sarA* mutant strains at various phases of growth. The probes used for hybridization were *icaR* and *icaA* for biofilm phenotype-related genes. (C) Northern blots of the regulatory locus (*agr* RNAIII), protein A (*spa*), α -hemolysin (*hla*), and V8 protease (*sspA*) genes for the wild-type, *teg49* mutant (ALC7907), *teg49* mutant with pEPSA5::*teg49* (ALC7912), and isogenic *sarA* mutant strains from various growth phases as indicated. All the strains containing pEPSA5 and its derivatives were grown in the presence of 2% xylose for the induction of *teg49*. A total of 10 μ g of cellular RNA from various phases of growth was loaded onto each lane. The 23S and 16S rRNAs of an ethidium bromide-stained gel used for blotting are shown as the loading control. The numbers beside the gels are OD₆₀₀ values.

The effect of *teg49* on virulence genes, such as *agr*, *spa*, *hla*, and *sspA*, in the SH1000 background was also examined. As shown in Fig. 4C, RNAIII of the *agr* locus was moderately increased in the complemented mutant ($27\% \pm 5\%$) versus the parent (set at 100%) and the *teg49* mutant ($9\% \pm 5\%$), while RNAIII expression was much lower in the *sarA* deletion mutant ($56\% \pm 5\%$) than in the parental strain, SH1000. However, the effect of *teg49* on *spa*, *hla*, and *sspA* was more subtle, with lower *hla* expression and higher *spa* expression in the *teg49* mutant versus the parent; these phenotypes are inconsistent with higher RNAIII expression. A slight decrease in *sspA* mRNA was detected in the mutant versus the parent, concordant with a lack of change in the SarA protein level in the mutant. As expected, the control *sarA* deletion mutant expressed lower levels of *agr* and *hla* and higher *spa* and *sspA* levels versus the parent (Fig. 4C). Plate-based phenotypic assays were performed to determine the zone of clearance on tryptic soy agar (TSA) containing sheep blood to determine the overall hemolysin activity. As shown in Table 1, there were very slight changes in the zone of clearances for hemolysis: 15 ± 2 mm for ALC7907 (*teg49* mutant) compared to 18 ± 2 mm for the wild type. Further characterization indicated that there was no growth difference

TABLE 1 Plate assays for hemolysins and proteases

Strain ^a	Zone of clearance (mm)	
	Sheep blood agar	5% skim milk
SH1000 (wt)	18 ± 2	5 ± 1
ALC7907 (teg49 KO)	15 ± 2	4 ± 1
ALC7910 (ALC7907 containing pEPSA5)	16 ± 2	4 ± 1
ALC7912 (ALC7907 containing pEPSA5 plus teg49)	15 ± 2	5 ± 1
ALC2732 (<i>sarA</i> KO)	12 ± 2	15 ± 1.5

^aKO, knockout.

between the wild-type and the teg49 mutant strains. In addition, DNA sequence analysis of the *sarA* loci of both strains suggested that there were no additional base changes in the wild-type and teg49 mutant strains. Therefore, the observed results from these experiments were likely attributable to the deletion of the teg49 region within the *sarA* locus.

RNA-Seq analysis of the teg49 mutant. As deletion of teg49 did not significantly alter SarA protein expression and overexpression of teg49 seemed to augment *agr* expression independently of SarA, we wanted to gain insight into the overall spectrum of genes controlled by teg49 via transcriptional profiling using Illumina RNA-Seq. To refine the expression profile of the teg49 mutant, a minimum read value of 50 reads per kilobase per million (RPKM) and a 4-fold change were considered to reduce the large number of genes attributable to teg49 deletion. In addition, phage-borne genes were also eliminated from our analysis. Using 4-fold change as the cutoff, transcriptional profiling by RNA-Seq revealed that 155 genes were upregulated in the teg49 mutant versus the wild-type strain, while 140 genes were downregulated. As the *sarA* P3 mRNA was altered in the teg49 mutant (Fig. 3B), the RNA-Seq profile of teg49 was further refined by subtracting *sarA*-mediated genes of SH1000 deduced from the RNA-Seq data of the *sarA* mutant. In all, 133 genes were upregulated for expression and 97 genes were downregulated in the teg49 mutant versus the wild-type strain (see Tables S2 and S3 in the supplemental material). There were 47 increases and 70 decreases in metabolism- and enzyme-related transcripts, 33 increases and 13 decreases in cell wall- and transport-related gene products, 40 increases and 3 decreases in mRNAs involved in cellular processes and regulatory and virulence factors, and 13 increases and 11 decreases in expression of genes with unknown functions in the teg49 mutant compared to the wild-type strain. Table 2 shows a few selected categories of genes, such as those involved in cellular function, regulatory processes, and virulence factors, that were altered in the teg49 mutant versus the parental strain. Interestingly, two known regulatory genes (*saeRS* and *lytS*), as well as four unknown genes, were upregulated in the teg49 mutant versus the parent, while three putative regulatory genes were downregulated. Notably, the *saeRS* regulatory system, which is not a part of the *sarA* regulon, was upregulated (~104-fold for *saeR* and ~52-fold for *saeS* transcripts) in the teg49 mutant versus the parent, indicating strong *saeRS* repression by teg49. The exact role of this regulatory relationship is not clear and is under investigation. Among 33 upregulated virulence genes in the teg49 mutant, 13 genes are related to toxins (e.g., *hlgA*, *hlgB*, *lukS*, *lukF*, SAOUHSC_00354, SAOUHSC_00383, SAOUHSC_00392 to SAOUHSC_00395, SAOUHSC_01124, SAOUHSC_01125, and SAOUHSC_01127), 7 genes are related to autolysis and proteases (e.g., *IrgA*, SAOUHSC_02166, SAOUHSC_02170, SAOUHSC_02023, SAOUHSC_02019, and SAOUHSC_01576), and 13 genes are related to cell wall factors (e.g., *map*, *sbi*, SAOUHSC_02167, SAOUHSC_02160, SAOUHSC_01114, SAOUHSC_01115, SAOUHSC_01110, and SAOUHSC_01112), while the expression of one virulence gene (*smc*) is reduced among downregulated genes in the teg49 mutant (Table 2). Consistent with our finding that the SarA protein level did not change significantly between the teg49 mutant and the wild type, the RNA-Seq data revealed no significant differences in the expression of several well-known *sarA*-regulated genes between the isogenic mutant strains. For instance,

TABLE 2 Upregulated and downregulated expression of selected genes in the *teg49* mutant versus the wild type

Gene designation	Gene name or description	Expression value		
		Wild-type SH1000	ALC7907 <i>teg49</i> mutant	Fold change
Upregulated genes				
Cellular process and regulatory systems				
SAOUHSC_01575	Helix-turn-helix domain-containing protein	0	166	166
SAOUHSC_02053	Transcriptional activator RinB-like protein	0	143	143
SAOUHSC_00715	Response regulator; SaeR	298	31,113	104.40
SAOUHSC_02077	Mga helix-turn-helix domain protein	0	72	72
SAOUHSC_02235	Repressor	0	55	55
SAOUHSC_00714	Sensor histidine kinase; SaeS	425	22,405	52.72
SAOUHSC_00230	Two-component sensor histidine kinase	92	384	4.17
Virulence factors				
SAOUHSC_02167	Staphylococcal complement inhibitor	10	32,147	3214.7
SAOUHSC_02160	Map domain protein	27	20,766	769.11
SAOUHSC_02160	MHC ^a class II analog protein (Map)	30	20,205	673.5
SAOUHSC_00401	Staphylococcal complement inhibitor; SCIN	77	36,003	467.57
SAOUHSC_01115	Staphylococcal complement inhibitor	26	7,600	292.30
SAOUHSC_01114	Fibrinogen-binding protein	26	7,399	284.57
SAOUHSC_02166	Putative holing-like protein	0	254	254
SAOUHSC_02706	Immunoglobulin G-binding; Sbi	19	3,767	198.26
SAOUHSC_02170	Peptidoglycan hydrolase	0	193	193
SAOUHSC_02708	Gamma-hemolysin H-gamma-II subunit; HlgA	12	1,902	158.5
SAOUHSC_01110	Fibrinogen-binding protein-like protein	21	3,142	149.61
SAOUHSC_01112	Formyl peptide receptor-like 1-inhibitory protein	34	4,726	139
SAOUHSC_00354	Staphylococcal/streptococcal toxin, beta-grasp domain	11	1,119	101.72
SAOUHSC_02710	Leukocidin F subunit; HlgB	37	3,416	92.32
SAOUHSC_02243	Leukotoxin; LukS	84	5,299	63.08
SAOUHSC_02171	Staphylokinase	0	55	55
SAOUHSC_02023	Bifunctional autolysin	0	42	42
SAOUHSC_02019	Autolysin	0	34	34
SAOUHSC_01576	Exonuclease family protein	0	27	27
SAOUHSC_02241	Leukotoxin; LukF	130	3,494	26.87
SAOUHSC_00393	Superantigen-like protein 8	4	91	22.75
SAOUHSC_00816	Extracellular matrix and plasma binding protein; Ssp	20	407	20.35
SAOUHSC_00394	Superantigen-like protein 9	4	74	18.5
SAOUHSC_00383	Superantigen-like protein 1	27	464	17.18
SAOUHSC_00191	Staphylococcal complement inhibitor	5	68	13.6
SAOUHSC_00395	Superantigen-like protein 10	11	132	12
SAOUHSC_01127	Superantigen-like protein	10	100	10
SAOUHSC_01125	Superantigen-like protein	8	79	9.87
SAOUHSC_00392	Superantigen-like protein 7	8	72	9
SAOUHSC_00192	Staphylocoagulase; Coa	7	46	6.57
SAOUHSC_01124	Superantigen-like protein	11	68	6.18
SAOUHSC_00241	Cold shock protein B	7,372	30,223	4.09
SAOUHSC_00232	Murein hydrolase regulator; LrgA	141	602	4.26
Downregulated genes				
Cellular process, transcriptional regulators, and virulence factors				
SAOUHSC_01196	Fatty acid biosynthesis transcriptional regulator	1,075	115	9.34
SAOUHSC_01204	SMC domain-containing protein	209	35	5.97
SAOUHSC_01206	DNA-binding protein	259	47	5.51

^aMHC, major histocompatibility complex.

some of the regulatory genes known to be repressed by SarA, e.g., *sarT* (1 versus 2), *sarU* (1 versus 1), and *sarV* (117 versus 93) did not differ in expression read values (RPKM) between the *teg49* mutant and the wild type, implying that there may be two distinct pathways for the regulation of target genes by SarA and *teg49* sRNAs in *S. aureus*.

Validating the expression of selective target genes of *teg49* sRNA. To validate our RNA-Seq data, we analyzed by Northern analysis six known and putative genes that were altered in the *teg49* mutant but not in the *sarA* mutant (SAOUHSC_00401, SAOUHSC_02160, SAOUHSC_02167, SAOUHSC_02841, *saeR*, and *lytS*). As shown in

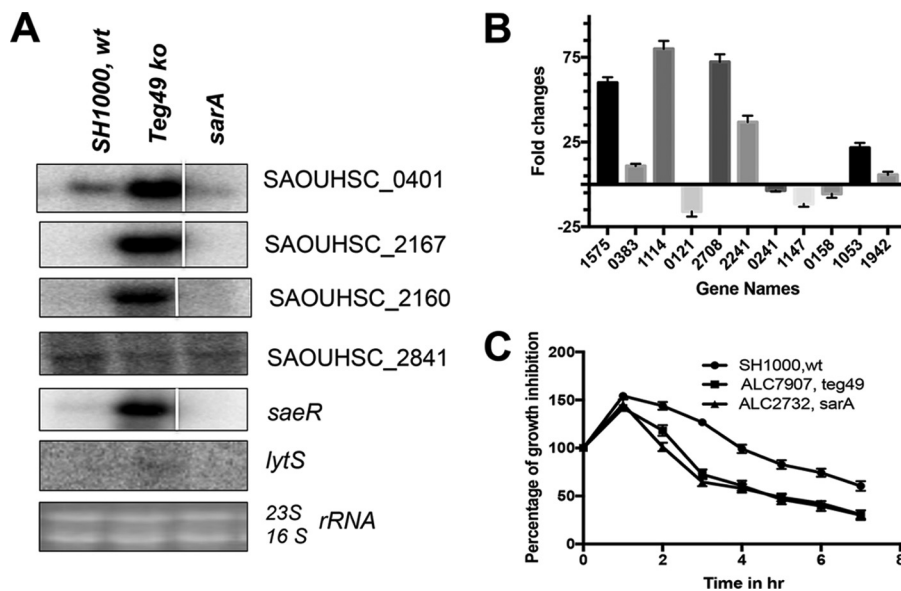


FIG 5 Validation of RNA-Seq data by Northern blot and phenotypic assays. (A) Northern blots of RNA-Seq data on deduced *teg49* target genes, including SAOUHSC_0401 (467-fold upregulated), SAOUHSC_02167 (3,214-fold upregulated), SAOUHSC_02160 (769-fold upregulated), SAOUHSC_02841 (32-fold downregulated), *saeR* (104-fold upregulated), and *lytS* (4-fold upregulated) for the wild-type, *teg49* mutant (ALC7907), and isogenic *sarA* mutant strains at the exponential phase of growth. A total of 10 μ g of cellular RNA was loaded onto each lane. The 23S and 16S bands of the ethidium bromide-stained gel used for blotting are shown as the loading control. The spliced images were taken from different regions of the same image. (B) Thirteen randomly selected RNA-Seq-analyzed genes, along with the *gyrB* control, were selected for qRT-PCR using total RNA isolated from the respective strains at the exponential phase of growth. The data were normalized against *gyrB* as the reference transcript for qRT-PCR. All the numbers on the x axis are the gene names from the *S. aureus* strain NCTC8325 genome (SAOUHSC). (C) Effect of *teg49* inactivation on penicillin-induced lysis or growth inhibition. Penicillin G-induced lysis of wild-type SH1000, *teg49* mutant (ALC7907), and isogenic *sarA* mutant (ALC2732 as the control) strains was measured as a decrease in the optical density at 650 nm over time. Penicillin G (0.04 μ g/ml, or \sim 10-fold subinhibitory concentration) was added to early-exponential-phase growing cultures ($OD_{650} \approx 0.25$), and changes in the OD_{650} were monitored over a 7-h period. The percentage of growth inhibition or lysis by penicillin G over time was plotted and was calculated as the OD over time divided by the OD at the time penicillin G was added multiplied by 100. The experiments were repeated at least three times. The results are expressed as means and standard errors of the mean.

Fig. 5A, the expression of the SAOUHSC_401, SAOUHSC_02167, and SAOUHSC_2160 mRNAs was significantly elevated in the *teg49* mutant versus the wild type, consistent with the RNA-Seq data (read values of 36,003 versus 77, 32,147 versus 10, and 20,766 versus 27, respectively, for SAOUHSC_401, SAOUHSC_02167, and SAOUHSC_2160) (Table 2). In contrast, the expression of the SAOUHSC_02841 transcript was reduced in the *teg49* mutant, concordant with a 32-fold reduction in read values (RPKM) in the *teg49* mutant versus the parental strain (see Table S2 in the supplemental material). Similarly, the expression of two regulatory genes, *saeR* and *lytS*, was found to be increased in the *teg49* mutant versus the parent by Northern analysis (Fig. 5A), in agreement with the results of RNA-Seq (Table 2). To further validate the RNA-Seq results, quantitative RT-PCR was performed with 13 putative genes, using the *gyrB* gene as the control (Fig. 5B). Among these analyzed genes, nine were upregulated, as determined by RNA-Seq (see Table S2 in the supplemental material) (SAOUHSC_02235, SAOUHSC_01575, SAOUHSC_00383/*set1* nm, SAOUHSC_01925, SAOUHSC_01114, SAOUHSC_02708/*hlgA*, SAOUHSC_02241/*lukF*, SAOUHSC_01053/*mntH*, and SAOUHSC_01942/*splA*) while four were downregulated (SAOUHSC_00121/*capH*, SAOUHSC_00241/*rbsU*, SAOUHSC_01147/*murD*, and SAOUHSC_00158), covering a wide range of genetic pathways ranging from metabolism to proteins with unknown functions (see Table S3 in the supplemental material). qRT-PCR analysis confirmed changes in gene expression in the *teg49* mutant (Fig. 5B), with the exception of two genes (SAOUHSC_02235 and SAOUHSC_01925) that failed to produce any product either by qRT-PCR or by normal PCR using the first-strand

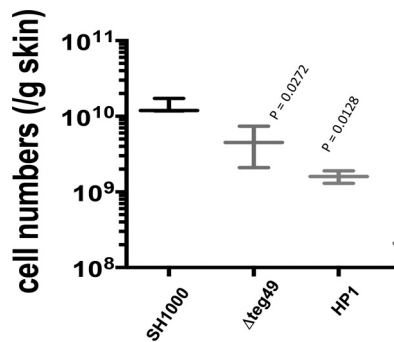


FIG 6 The teg49 and HP1 mutants exhibited reduced virulence in a mouse model of skin abscess infection. Mice (6 in each group) were challenged with $\sim 1 \times 10^8$ CFU of *S. aureus* SH1000 or its isogenic teg49 or HP1 mutant and observed daily for the presence of skin abscesses. Shown are the mean numbers of colonies counted per gram of infected skin tissue with standard errors of the mean. The mean counts per gram of tissue for the teg49 and HP1 mutants were considered to be statistically significantly different from that of the parent.

synthesized DNA (cDNA) as the template, indicating that detection of these two genes by RNA-Seq may be due to artifacts. Thus, Northern blots and qRT-PCR results validated the RNA-Seq data and indicated that teg49 sRNA has an important role in regulating the stability of these transcripts. Whether teg49 is involved directly or indirectly has yet to be determined. The increase in transcript levels for genes encoding putative autolysin (SAOUHSC_02019 and SAOUHSC_02023), putative peptidoglycan hydrolase (SAOUHSC_02170), a putative holin-like protein (SAOUHSC_02166), and regulator-like LrgA in the teg49 mutant (but not in the *sarA* mutant) suggested that teg49 may have some role in autolysis of *S. aureus*. Accordingly, we tested the teg49 mutant for susceptibility to penicillin-induced lysis (Fig. 5C). Penicillin G (0.04 $\mu\text{g/ml}$; the MIC for strain SH1000 is $\leq 0.004 \mu\text{g/ml}$) was added to a growing culture at the early exponential phase of growth ($\text{OD}_{650} \sim 0.25$), and the OD_{650} was monitored over a 7-h period. As shown in Fig. 5C, the teg49 mutant exhibited sensitivity to penicillin-induced lysis compared to the wild-type SH1000. As a positive control, the *sarA* mutant displayed high sensitivity to penicillin-induced lysis, consistent with previously published data (36). This sensitivity to penicillin-induced lysis in the teg49 mutant is notable because the SarA protein level in the teg49 mutant was only slightly reduced compared with the wild type (Fig. 3D). Overall, this phenotypic observation validates the changes in the levels of transcription of autolysis-related genes in the teg49 mutant compared with the parent.

Murine model of skin abscess with the teg49 mutant. To seek *in vivo* correlation, the virulence of the teg49 mutant, along with those of the wild type and the HP1 mutant of teg49 (32), was evaluated in a mouse skin abscess model of infection (Fig. 6). Using the number of CFU per gram of skin abscess tissue as a readout, the results indicated that there was a significant difference ($P \approx 0.0272$) between the bacterial cell density of teg49 mutant and those of the wild-type strains at 5 days after initial infection. Similarly, mutation in HP1 of teg49, a crucial structure of teg49 (32), also showed a reduced bacterial load ($P \approx 0.0128$) compared to the wild-type strain. It should be mentioned that, despite the finding that teg49 did not affect the overall SarA expression in a significant way, RNA-Seq studies suggested that teg49 might affect virulence genes independently of SarA. This *in vivo* study using the murine model of cutaneous abscess seems to support that hypothesis.

DISCUSSION

The discovery of sRNAs in bacteria in the last 2 decades has provided new insights into gene regulation. sRNAs have been found to be ubiquitous and represent the most abundant class of posttranscriptional regulators in prokaryotes (21–23). Most of the sRNAs act by base pairing with target mRNAs. However, the majority of sRNA studies have been limited to *Escherichia coli* and other Gram-negative bacteria (23). With the

exception of RNAlII, most of the sRNA studies in Gram-positive bacteria, including *S. aureus*, are not well delineated mechanistically (22). The RNAlII molecule, a 516-nt-long RNA, is an effector molecule of the *agr* system and activates translation of the *hla* gene product (26) and stabilizes *mgrA* transcripts (27), as well as inhibiting translation of many transcripts, such as *rot*, *sa1000* (fibrinogen binding protein), *sa2261* (ABC transporter), *spa* (protein A), *lytM* (peptidoglycan hydrolase), *map* (major histocompatibility complex class II-analogous protein), and *coa* (coagulase) (21, 22). Thus, RNAlII of the *agr* system has established the role of sRNA in stability and translation of mRNA in *S. aureus*.

Besides *agr*, *sarA* is another major regulatory locus involved in the expression of toxins, enzymes, and cell wall adhesins. The *sarA* locus is peculiar in that the 372-bp *sarA* coding region is preceded by an ~850-bp-long 5' UTR that consists of three distinct promoters, yielding three overlapping transcripts (16, 17). However, complementation studies suggest that the 5' UTR may play an important role in optimal expression of the SarA protein (20). Recent identification of two sRNAs in this region by RNA-Seq analysis (25) provided the impetus to ascertain the role of sRNA teg49 in gene regulation in SarA-dependent and SarA-independent manners (32).

In this report, we have shown via mutation analysis of the -35 and -10 promoters of the *sarA* locus that teg49 is most likely produced and processed from the P3 *sarA* transcript (Fig. 1). Most notably, in the absence of teg49 in SH1000, the transcription of P3 *sarA* mRNA ceased (Fig. 3B) but was restored upon *trans*-complementation from a plasmid expressing teg49 in the teg49 mutant (ALC7912), thus indicating that teg49 has an important role in the stability of the P3 *sarA* transcript. Surprisingly, the overall SarA level was, at best, slightly altered (Fig. 3D) despite the relative absence of the *sarA* P3 and, to a certain extent, *sarA* P2 transcripts in the teg49 mutant, signifying that overall SarA expression is mostly due to the contribution of the P1 *sarA* transcript in *S. aureus*. Previous studies have shown in strain Newman that the production of teg49 was *cshA* dependent (32). This result was also confirmed in the SH1000 background. Traditionally, CshA has been known to be involved in ribosome biogenesis, ribosome assembly, and mRNA decay in a degradosome involving RNase J, RNase Y, and polynucleotide phosphorylase (PNPase) (37). Our unpublished *in vitro* assay with purified CshA and *in vitro*-transcribed P3 *sarA* mRNA demonstrated that CshA can bind the *sarA* P3 transcript and protect it from endonuclease (e.g., RNase III). In this regard, we surmise that CshA may be involved in the initial stability and eventual processing of the *sarA* P3 transcript by an RNase to yield teg49 sRNA. Surprisingly, inactivation of Hfq, an sRNA chaperone well described in Gram-negative bacteria, did not yield any alterations in the levels of transcripts of three analyzed sRNAs (i.e., teg49, teg23, and teg35). This finding indicated that Hfq does not have a major role in stabilizing sRNA in *S. aureus*, consistent with other reports of Gram-positive bacteria (23).

Analysis of the putative RNase mutants in the JE2 mariner transposon library indicated that RNase III, an endoribonuclease that cleaves double-stranded RNA (38, 39), may be required for processing of the *sarA* P3 transcript to produce teg49. The specificity of RNase III in this cleavage was demonstrated with teg23, another sRNA known to be stabilized by CshA, while the control, teg35, an sRNA not stabilized by CshA (34), was not altered in the *mnc* mutant. Previous studies have shown that RNase III is normally involved in regulating the turnover of mRNAs and noncoding RNAs (40, 41). RNase III also likely targets the 5' overlapping regions of divergent mRNAs to generate species with shorter or even leaderless 5' UTRs (42).

Among several other mutants tested for putative endoribonuclease activity to cleave *sarA* P3 mRNA (Fig. 2A), we found that inactivation of the conserved hypothetical-protein genes (e.g., SauUSA300_1184, SauUSA300_2328, and SauUSA300_1692), ABC permease gene (SauUSA_308), and polyribonucleotide transferase (*pnp*) gene did not have any effect on expression of teg49. Only inactivation of three genes (*nrdD*, *rny*, and endo-RNase L-PSP) showed increased expression; the reason for this increase is not clear at this point. Notably, RNase E, an important part of the degrado-

some that processes mRNA in many Gram-negative bacteria, is absent in *S. aureus*, while RNase Y (encoded by *rny*), which is involved in processing of monophosphorylated RNA (43), appears to have a role in destabilizing *teg49* (Fig. 2A). Collectively, these results indicated that endoribonucleases are likely involved in the generation and stabilization of *teg49* sRNA. Consistent with a lack of major alteration in the overall level of the SarA protein, a major player in regulating biofilm formation, in the *teg49* mutant, there was no major change in biofilm formation in the *teg49* mutant. It should be noted that regulation of biofilm formation is a complex process, and several known regulatory systems, such as Rbf, SarX, and SarR, also participate in regulation at the transcriptional level in *Staphylococcus* species (44). In contrast to the biofilm-related genes (e.g., *icaA* and *icaR*), the *spa* transcript is upregulated while the *hla* and *sspA* transcripts are downregulated in the *teg49* mutant, as supported by RNA-Seq and Northern analyses, accompanied by slight phenotypic alterations in zones of clearance for hemolysis and proteases (Table 1). This pattern of regulation is inconsistent with moderate upregulation of RNAlII and mild alteration of the SarA protein level in the *teg49* mutant. Coincidentally, we determined by RNA-Seq that *saeRS*, a genetic locus not directly linked to *agr* and *sarA*, is significantly upregulated in the *teg49* mutant. Elevated *saeRS* would be expected to result in elevated *spa* and *hla* and curtailed *sspA* expression, which does not completely explain the *teg49* virulence genotype/phenotype that we have observed. It is conceivable that inactivation of *teg49* leads to a combination of regulatory events (e.g., elevated *agr* and *sae* and other factors) that may be able explain what we observed here in the *teg49* mutant.

By setting various criteria, such as minimum read values, discarding phage-borne genes, eliminating *sarA*-regulated genes, and designating 4-fold changes for significance, our RNA-Seq analysis also showed that 133 and 97 genes are up- and downregulated, respectively, in the *teg49* mutant compared to the wild type. Several virulence genes, such as those encoding complement inhibitor proteins (SAOUHSC_02167, SAOUHSC_00401, SAOUHSC_01115, SAOUHSC_02160, *map*, and *sbi*), leukotoxins and superantigen-like proteins, and fibrinogen-binding protein-like proteins, were altered due to *teg49* deletion in the *S. aureus* genome (Table 2).

It has been shown that antisense base pairing of *sbi* mRNA (encoding an immunoglobulin binding protein) with SprD, an sRNA expressed from an *S. aureus* pathogenicity island (PI Φ), led to an impaired host immune response (30). It would be interesting to investigate the existence of similar mechanisms between *teg49*-regulated virulence genes and *teg49* in the future. Besides direct base-pairing with target mRNA, several other mechanisms, including dual-function sRNA that acts as an antisense molecule and codes for a small peptide (e.g., Hld in RNAlII), have been proposed to act on the same or other pathway genes, and also riboswitches that exhibit a structured receptor domain specifically recognized by a small molecule or metabolite (22, 45). Together, our data suggest that *teg49* sRNA has a regulatory role in *S. aureus*, but the exact mode of regulation is yet to be determined.

Overall, our results presented here indicated that *teg49* sRNA is processed and produced from the *sarA* P3 transcript of the *sarA* locus and that its stability depends on the *csfA* and *rnc* gene products. Inactivation of *teg49* has no major effect on the overall level of SarA expression, and *teg49* appears to be required for the stability of the P3 *sarA* transcript. Transcriptome profiling indicated about 230 genes with at least a 4-fold change were affected in the *teg49* mutant in a *sarA*-independent manner. The sRNA *teg49* appears to be involved in penicillin-mediated lysis but not in biofilm formation. A mouse skin abscess model of infection revealed a modest but significant reduction in the bacterial load in the infected skin tissue, thus demonstrating that *teg49* plays a noticeable role in virulence gene regulation in *S. aureus*. Whether *teg49* acts as a riboswitch in *S. aureus* is not clear at this point. Whether *teg49* can be considered a target for the development of novel antibacterial compounds to overcome the current mechanisms of resistance remains to be determined.

TABLE 3 Bacterial strains and plasmids used in this study

<i>S. aureus</i> strain or plasmid	Description ^a	Reference or source
Strains		
RN4220	Restriction-deficient transformation recipient	52
SH1000	Wild-type laboratory strain with a functional <i>rsbU</i> ⁺ derivative of the 8325-4 <i>rsbU</i> -defective strain	53
ALC7907	teg49 mutant of SH1000; chromosomal deletion of 204-bp teg49 from bp 182 to 386 from the ATG start codon of the <i>sarA</i> gene	This study
ALC7910	ALC7907 containing an empty xylose-inducible vector, pEPSA5	This study
ALC7912	ALC7907 containing pEPSA5 carrying 183-bp teg49 fragment DNA under a xylose-inducible promoter	32
ALC8070	teg48 mutant of SH1000; chromosomal deletion of 68 bp from the teg48 region of the <i>sarA</i> locus	This study
ALC8372	SH1000 chromosomal P ₂ promoter mutant at the -35 and -10 sequences of the <i>sarA</i> locus	This study
ALC8373	SH1000 chromosomal P ₃ promoter mutant at the -35 and -10 sequences of the <i>sarA</i> locus	This study
ALC8374	SH1000 chromosomal P ₁ promoter mutant at the -35 and -10 sequences of the <i>sarA</i> locus	This study
ALC 8441	ALC8373 mutated P ₃ promoter chromosomally repaired to wild-type P ₃ promoter at the -35 and -10 sequences of the <i>sarA</i> locus	This study
ALC 2732	<i>sarA</i> mutant of SH1000; <i>sarA::erm</i>	14
AM 1262	Complemented with <i>sarA</i> into the <i>geh</i> locus on chromosome of the <i>sarA</i> mutant of SH1000; <i>sarA::erm</i>	14
ALC8243	<i>rnc</i> or RNase III mutant of SH1000; <i>rnc::erm</i>	This study
ALC8445	Complemented ALC8243 with pSK236 carrying a 1.5-kb fragment containing the <i>rnc</i> gene region	This study
ALC8235	<i>cshA</i> mutant of SH1000, <i>chsA::kan</i>	This study
ALC8245	<i>hfq</i> mutant of SH1000; <i>hfq::erm</i>	This study
NE1494	<i>rnc</i> RNase III of JE2 (SAUUSA300_01126)	33
NE1707	SAUSA300_1184:: <i>erm</i> of JE2	33
NE0581	<i>nrdD</i> mutant of JE2; <i>nrdD::erm</i> (SAUUSA_2551)	33
NE0259	<i>pnpA</i> mutant of JE2; <i>pnpA::erm</i> (SAUSA300_1167)	33
NE1205	<i>nrdG</i> mutant of JE2; <i>nrdG::erm</i> (SAUSA_2550)	33
ALC8428	<i>rnaseY</i> mutant of JE2 constructed by transduction from Newman <i>rnaseY::erm</i> (SAUSA300_01179)	This study
NE0291	SAUSA300_2328:: <i>erm</i> of JE2	33
NE1079	SAUSA300_2021:: <i>erm</i> of JE2	33
NE0458	<i>xseA</i> mutant JE2; <i>xseA::erm</i> (SAUSA300_1472)	33
NE1340	SAUSA300_1692:: <i>erm</i> of JE2	33
NE0501	<i>rnr</i> mutant of JE2; <i>rnr::erm</i> (SAUSA300_0764)	33
NE0404	Endo-RNase L-PSP mutant of JE2; endo-RNase L-PSP:: <i>erm</i> (SAUSA300_0474)	33
NE0931	SAUSA300_0308:: <i>erm</i> of JE2	33
Plasmids		
pMAD	<i>E. coli</i> - <i>S. aureus</i> shuttle vector containing temperature-sensitive origin of replication, <i>bgaB</i> ; Erm ^r Ap ^r	47
pEPSA5	<i>E. coli</i> - <i>S. aureus</i> xylose-inducible shuttle vector containing xylose-inducible promoter for conditional expression of the desired gene; Cm ^r Ap ^r	32
pEPSA5::teg49	pEPSA5 containing 196-bp teg49 sRNA region	32
pSK236	Shuttle vector containing pUC19 cloned into the HindIII site of pC194	14

^aErm, erythromycin; Ap, chloramphenicol; Cm, chloramphenicol.

MATERIALS AND METHODS

Bacterial strains, plasmids, and culture media. The bacterial strains and plasmids used in this study are listed in Table 3. *S. aureus* strain RN4220, a restriction-deficient derivative of strain 8325-4, was used as the initial recipient for the transformation of plasmid constructs. The *S. aureus* strains were grown in tryptic soy broth (TSB) or on TSA supplemented with antibiotics when necessary (5 μg/ml of erythromycin and 10 μg/ml of chloramphenicol). The cells were grown with continuous aeration in a shaker at either 37°C or the required permissive temperatures. Luria-Bertani (LB) broth or agar, supplemented with suitable antibiotics when necessary (100 μg/ml of ampicillin and 40 μg/ml of kanamycin), was used for growing *E. coli*. Growth was monitored by measuring changes in turbidity at 600 nm in a spectrophotometer (Spectronic 20D).

Genetic manipulation. Standard procedures for DNA manipulations were performed using routine cloning procedures (46). Mutagenesis of various *sarA* promoters (P₂, P₃, and P₁) was performed using pCR2.1 containing a P₂ *sarA* fragment flanking BamHI sites at both ends as a template and various mutagenized primer pairs as listed in Table S1 in the supplemental material (P₂ *sarA*, -35 AGCAAA to CCCCAC and -10 TAATAT to CCACTC; P₃ *sarA*, -35 AGTGAT to CCCAAA and -10 GGGTAT to CCACTC; and P₁ *sarA*, -35 TTTACT to CCCCAA and -10 TATAAT to CCACTC). PCR-mediated plasmid mutagenesis was performed using *Pfu* and *Taq* polymerases, and clones were authenticated by DNA sequencing. The 1.5-kb BamHI fragments containing various individual promoter mutations were cloned into the BamHI site of the temperature-sensitive shuttle vector pMAD (47). The recombinant pMAD plasmids were first electroporated into strain RN4220 and then into *S. aureus* strain SH1000 for construction of various mutants. Construction, selection, and authentication of the putative mutants were performed as described previously (46, 47). These mutant strains were labeled ALC8372 (P₂m), ALC8373 (P₃m), and ALC8374 (P₁m) for *sarA* P₂, P₃, and P₁ promoter knockout mutants, respectively. To restore the promoter

in the P₃m promoter knockout strain, a 1.5-kb fragment containing the native P3 *sarA* fragment was cloned into pMAD and transformed into strain ALC8373 to construct a revertant P₃m/P₃wt strain, ALC8441, following the same procedure as previously described for mutant strain construction. Construction of *rnc::erm* (ALC8243), *cshA::kan* (ALC8235), *hfq::erm* (ALC8245) of SH1000 and *rny::erm* (ALC8428) of JE2 was performed by phage transduction from the respective Newman background mutant strains. To complement the *rnc* mutation, a 1.5-kb DNA fragment encompassing the *rnc* gene region was cloned in shuttle plasmid pSK236 and transformed into ALC8243 (*rnc::erm*) to construct a *trans*-complemented strain (ALC8445).

Construction of the teg49 mutant was performed using the same PCR-mediated method of mutagenesis with the primers used in Table S1 in the supplemental material to delete 204 bp from bp 385 to 182 upstream from the ATG start codon of the *sarA* gene using pCR2.1 carrying a 2.3-kb fragment encompassing the *sarA* locus as the template. A 2.2-kb DNA fragment containing the deletion was cloned into pMAD to construct the teg49 deletion mutant (ALC7907), as described previously for the construction of various promoter mutants. Final authentication of various mutant strains was performed by DNA sequencing of the PCR products and Northern hybridization. Complementation of the teg49 mutant was performed in *trans* using pEPSA5::teg49 in the presence of 2% xylose in broth (32).

Isolation of total cellular RNA and Northern blot hybridization. Isolation of total cellular RNA from various growth phases and subsequent analysis by Northern blot hybridization were performed as described previously (46). DNA fragments containing the open reading frames of *sarA*, *icaA*, *icaR*, *spa*, *hla*, and *sspA* or sRNA teg49, teg23, and teg35 and other RNA-Seq-validated genes were amplified by PCR or excised from the plasmids containing the desired genes with restriction endonucleases and then gel purified. For detection of specific transcripts, gel-purified DNA probes were radiolabeled with [α -³²P]dCTP by using the random-primed DNA-labeling kit (Roche Diagnostics GmbH) and hybridized under aqueous-phase conditions at 65°C. The blots were subsequently washed, exposed to a phosphorimager screen, and scanned. Each of the experiments was repeated at least three times independently.

Western blotting and immunodetection. Whole-cell extracts from *S. aureus* wild-type SH1000 or various mutant strains were prepared from cells grown to different growth phases, as described previously (46). The concentration of total proteins from clear lysates was determined by using a Pierce bicinchoninic acid (BCA) protein assay kit (Thermo Scientific, USA) using bovine serum albumin as the standard. Western blotting and detection with primary antibody (anti-SarA) and donkey anti-mouse secondary antibody conjugated with horseradish peroxidase (HRP) and enhanced chemiluminescence (ECL) Western blotting substrate (Thermo Scientific) were performed as described previously (46). The experiments were repeated at least three times independently.

Biofilm assay. Quantification of biofilm formation on abiotic surfaces was performed as described previously (35, 48). Briefly, *S. aureus* strains grown overnight in TSB were diluted (1:50) in TSB supplemented with 0.25% glucose. This cell suspension was used to inoculate sterile 96-well U-bottom polystyrene microtiter plates (Costar, Corning Inc., USA) in triplicate. After 24 h of incubation at 37°C, the wells were gently washed three times with water, air dried in an inverted position, and stained with 0.1% crystal violet dye in water for 15 min at room temperature. The wells were rinsed 3 or 4 times by submerging them in water, dried for several hours to overnight in an inverted position, and solubilized in 30% acetic acid in water for 15 min. The solubilized dye was transferred to flat-bottom microtiter plates, and the absorbance at 550 nm was determined (Infinite M1000 Pro; Tecan, Austria). Each assay was repeated at least three times in separate experiments.

Protease and hemolysin assays. A protease assay for all the tested strains was performed using TSA supplemented with 5% skim milk. Similarly, a hemolysis assay was done using 5% sheep blood TSA plates (Remel, Kansas, USA). Equal volumes (3 μ l) of equivalent optical density (OD₅₀₀) of various strains were spotted onto plates in triplicate and incubated for 20 to 36 h at 37°C. The zones of clearance from three independent experiments were measured and compared.

RNA-Seq experiments. Samples for RNA-Seq were prepared from the following strains: the wild-type SH1000, its isogenic derivative teg49 mutant (ALC7907), and the isogenic *sarA* mutant (ALC2732). Briefly, overnight cultures were diluted 1:100 in fresh TSB (initial OD₆₀₀ about 0.04 to 0.05) and grown at 37°C for 3 h. Two replicate cultures for each sample were grown, and total cellular RNAs from two biological replicates were extracted as described previously (32). RNA was quantified by using Qubit (Life Technologies), and RNA integrity was assessed with a 2100 Bioanalyzer (Agilent Technologies). A 1- μ g amount of total RNA was ribodepleted with a bacterial Ribo-Zero kit from Illumina. A TruSeq RNA stranded kit from Illumina was used for library preparation. The library quantity was measured with Qubit, and quality was assessed on a TapeStation on a DNA high-sensitivity chip (Agilent Technologies). The libraries were pooled at equimolarity and loaded at 2 nM for clustering. Oriented 50-base single-read sequencing was performed on an Illumina HiSeq 4000 sequencer, yielding a minimum of 9 million mapped reads per sample. Final RNA-Seq analysis and data analysis were carried out using previously described procedures (32). Statistical analyses were done in R v3.2.3 using the edgeR package (49) following a bioinformatics protocol described previously (50). Briefly, genes whose expression was not at least one read per million in two replicates of the samples were filtered out. Counts of the retained genes were normalized according to the weighted trimmed mean of M values (TMM) method. Read counts for each transcript in each sample were modeled according to a negative binomial (NB) distribution. Finally, pairwise comparisons between read libraries from various strains were performed with the exact test (49, 50) to detect differentially expressed transcripts. *P* values were corrected according to the false-discovery rate (FDR).

qRT-PCR analysis. qRT-PCR was performed as previously described (34). Briefly, cDNA was obtained using GoScript cDNA synthesis mix (Promega, USA) and DNase I-treated purified total RNA as a template.

Maxima SYBR green/ROX qRT-PCR master mix (Thermo Scientific) was used to generate standard curves for the cDNA concentration/crossing point (C_p) for the target genes and the reference gene, *gyrB*. The mean target transcriptional expression level for the three transcript measurements was calculated. The threshold cycle ($2^{-\Delta\Delta CT}$) method was used to calculate relative changes in gene expression, using triplicate samples. Applied Biosystems StepOne Plus software was used to analyze the qRT-PCR results. Control reaction mixtures containing master mix and primers but no cDNA were also analyzed.

Penicillin G-mediated lytic assay. The penicillin G-mediated lytic assay was performed as described previously (36). In brief, to assess the sensitivity of the teg49 mutant and its isogenic derivative strains, along with the *sarA* mutant, to penicillin, inoculations were done in TSB from overnight cultures to yield a starting OD_{650} of 0.05. Penicillin G was added to a concentration of 0.04 $\mu\text{g/ml}$ (the MIC determined for strain SH1000 is $\leq 0.0039 \mu\text{g/ml}$) at the early exponential phase of growth ($OD_{650} \approx 0.25$). Cultures were incubated at 37°C with shaking, and the OD_{650} was measured every hour for 7 h.

Murine cutaneous model of infection. A murine skin infection model was used to determine the effect of the teg49 mutation on virulence in the SH1000 background. Animal experiments were performed in accordance with a protocol approved by the Institutional Animal Care and Use Committee at the Geisel School of Medicine at Dartmouth, Hanover, NH. Female BALB/c mice were held, shaved on the back, and inoculated by subcutaneous injection in the right flank with 1×10^8 *S. aureus* bacteria in 50 μl of PBS, using a 23-gauge needle. The mice were weighed before inoculation, and abscess formation was monitored at 24-h intervals for 5 days. The sizes of the abscesses were calculated using a standard formula for area [$A = (\pi/2) \times \text{length} \times \text{width}$], as described previously (51). Dermonecrosis was scored as present or absent. Six mice per group were used for each bacterial strain or control group. After 5 days of infection, at which time abscesses were evident in most mice, the mice were sacrificed and abscess tissues were collected, weighed, homogenized in saline containing 0.1% Triton X-100, and plated in triplicate in mannitol salt agar for incubation at 37°C for 48 h to derive the number of CFU per gram of abscess tissue for various strains.

Statistical analyses. Statistics for the abscess or lesion area were performed using 1-way or 2-way analysis of variance (ANOVA), as indicated. The results are expressed as means \pm standard errors of the mean unless otherwise indicated. All data were analyzed using Graph Pad Prism 7. The data represent the standard errors of the means from at least three independent experiments with multiple replicates unless otherwise indicated. For normally distributed data, comparisons were tested with Student's *t* test.

SUPPLEMENTAL MATERIAL

Supplemental material for this article may be found at <https://doi.org/10.1128/IAI.00635-17>.

SUPPLEMENTAL FILE 1, XLSX file, 0.1 MB.

SUPPLEMENTAL FILE 2, PDF file, 0.2 MB.

SUPPLEMENTAL FILE 3, XLSX file, 0.1 MB.

SUPPLEMENTAL FILE 4, XLSX file, 0.1 MB.

ACKNOWLEDGMENTS

This work was supported by grants AI106937 from the National Institutes of Health (to A.C.) and 31003A_153474/1 from the Swiss National Science Foundation (to P.F.).

REFERENCES

- Crossley KB, Archer GL. 1997. The staphylococci in human disease. Churchill Livingstone, New York, NY.
- Lowy FD. 1998. *Staphylococcus aureus* infections. N Engl J Med 339: 520–532. <https://doi.org/10.1056/NEJM199808203390806>.
- Foster TJ. 2005. Immune evasion by staphylococci. Nat Rev Microbiol 3:948–958. <https://doi.org/10.1038/nrmicro1289>.
- Kennedy AD, DeLeo FR. 2009. Neutrophil apoptosis and the resolution of infection. Immunol Res 43:25–61. <https://doi.org/10.1007/s12026-008-8049-6>.
- Diep BA, Otto M. 2008. The role of virulence determinants in community-associated MRSA pathogenesis. Trends Microbiol 16:361–369. <https://doi.org/10.1016/j.tim.2008.05.002>.
- Cheung AL, Nishina KA, Trottonda M-P, Tamber S. 2008. The SarA protein family of *Staphylococcus aureus*. Int J Biochem Cell Biol 40:355–361. <https://doi.org/10.1016/j.biocel.2007.10.032>.
- Novick RP. 2003. Autoinduction and signal transduction in the regulation of staphylococcal virulence. Mol Microbiol 48:1429–1449. <https://doi.org/10.1046/j.1365-2958.2003.03526.x>.
- Ballal A, Ray B, Manna AC. 2009. *sarZ*, a *sarA* family gene, is transcriptionally activated by MgrA and is involved in the regulation of genes encoding exoproteins in *Staphylococcus aureus*. J Bacteriol 191:1656–1665. <https://doi.org/10.1128/JB.01555-08>.
- Arya R, Princy SA. 2016. Exploration of modulated genetic circuits governing virulence determinants in *Staphylococcus aureus*. Indian J Microbiol 56:19–27. <https://doi.org/10.1007/s12088-015-0555-3>.
- Kornblum J, Kreiswirth B, Projan SJ, Ross H, Novick RP. 1990. Agr: a polycistronic locus regulating exoprotein synthesis in *Staphylococcus aureus*, p 403–420. In Novick RP (ed), Molecular biology of the staphylococci. VCH Publishers, New York, NY.
- Novick RP, Geisinger E. 2008. Quorum sensing in staphylococci. Annu Rev Genet 42:541–564. <https://doi.org/10.1146/annurev.genet.42.110807.091640>.
- Cheung AL, Koomey JM, Butler CA, Projan SJ, Fischetti VA. 1992. Regulation of exoprotein expression in *Staphylococcus aureus* by a locus (*sar*) distinct from *agr*. Proc Natl Acad Sci U S A 89:6462–6466. <https://doi.org/10.1073/pnas.89.14.6462>.
- Kavanaugh JS, Horswill AR. 2016. Impact of environmental cues on staphylococcal quorum sensing and biofilm development. J Biol Chem 291:12556–12564. <https://doi.org/10.1074/jbc.R116.722710>.
- Ballal A, Manna AC. 2010. Control of thioredoxin reductase (*trxB*) transcription by SarA in *Staphylococcus aureus*. J Bacteriol 192:336–345. <https://doi.org/10.1128/JB.01202-09>.
- Dunman PM, Murphy E, Haney S, Palacios D, Tucker-Kellogg Wu S, Brown EL, Zagursky RJ, Shlaes D, Projan SJ. 2001. Transcriptional profiling based identification of *S. aureus* genes regulated by the *agr* and/or *sarA* loci. J

- Bacteriol 183:7341–7353. <https://doi.org/10.1128/JB.183.24.7341-7353.2001>.
16. Bayer MG, Heinrichs JH, Cheung AL. 1996. The molecular architecture of the *sar* locus in *Staphylococcus aureus*. *J Bacteriol* 178:4563–4570. <https://doi.org/10.1128/jb.178.15.4563-4570.1996>.
 17. Manna AC, Bayer MG, Cheung AL. 1998. Transcriptional analysis of different promoters in the *sar* locus in *Staphylococcus aureus*. *J Bacteriol* 180:3828–3836.
 18. Ballal A, Manna AC. 2009. Expression of *sarA*-family genes in *S. aureus* strains. *Microbiology* 155:2342–2352. <https://doi.org/10.1099/mic.0.027417-0>.
 19. Blevins JS, Beenken KE, Elasm MO, Hurburt BK, Smeltzer MS. 2002. Strain-dependent differences in the regulatory roles of *sarA* and *agr* in *Staphylococcus aureus*. *Infect Immun* 70:470–480. <https://doi.org/10.1128/IAI.70.2.470-480.2002>.
 20. Cheung AL, Bayer MG, Heinrichs JH. 1997. *sar* genetic determinants necessary for transcription of RNAII and RNAIII in the *agr* locus of *Staphylococcus aureus*. *J Bacteriol* 179:3963–3971. <https://doi.org/10.1128/jb.179.12.3963-3971.1997>.
 21. Guillot J, Hallier M, Felden B. 2013. Emerging functions for the *Staphylococcus aureus* RNome. *PLoS Pathog* 9:e1003767. <https://doi.org/10.1371/journal.ppat.1003767>.
 22. Tomasini A, Francois P, Howden BP, Fechter P, Romby P, Caldelari I. 2014. The importance of regulatory RNAs in *Staphylococcus aureus*. *Infect Genet Evol* 21:616–626. <https://doi.org/10.1016/j.meegid.2013.11.016>.
 23. Pitman S, Cho KH. 2015. The mechanisms of virulence regulation by small noncoding RNAs in low GC Gram-positive pathogens. *Int J Mol Sci* 16:29797–29814. <https://doi.org/10.3390/ijms161226194>.
 24. Carroll RK, Weiss A, Broach WH, Wiemels RE, Mogen AB, Rice KC, Shaw LN. 2016. Genome-wide annotation, identification, and global transcriptomic analysis of regulatory or small RNA gene expression in *Staphylococcus aureus*. *mBio* 7:e01990-15. <https://doi.org/10.1128/mBio.01990-15>.
 25. Beaume M, Hernandez D, Farinelli L, Deluen C, Linder P, Gaspin C, Romby P, Schrenzel J, Francois P. 2010. Cartography of methicillin-resistant *S. aureus* transcripts: detection, orientation and temporal expression during growth phase and stress conditions. *PLoS One* 5:e10725. <https://doi.org/10.1371/journal.pone.0010725>.
 26. Morfeldt E, Taylor D, von Gabain A, Arvidson S. 1995. Activation of alpha-toxin in *S. aureus* by *trans*-encoded antisense RNA, RNAIII. *EMBO J* 14:4569–4577.
 27. Gupta RK, Luong TT, Lee CY. 2015. RNAIII of the *Staphylococcus aureus agr* system activates global regulator MgrA by stabilizing mRNA. *Proc Natl Acad Sci U S A* 112:14036–14041. <https://doi.org/10.1073/pnas.1509251112>.
 28. Bohn C, Rigoulay C, Chabelskaya S, Sharma CM, Marchais A, Skorski P, Borezee-Durant E, Barbet R, Jacquet E, Jacq A, Gautheret D, Felden B, Vogel J, Bouloc P. 2010. Experimental discovery of small RNAs in *Staphylococcus aureus* reveals a riboregulator of central metabolism. *Nucleic Acids Res* 38:6620–6636. <https://doi.org/10.1093/nar/gkq462>.
 29. Xue T, Zhang X, Sun H, Sun B. 2014. ArtR, a novel sRNA of *Staphylococcus aureus*, regulates α -toxin expression by targeting the 5'-UTR of *sarT* mRNA. *Med Microbiol Immunol* 203:1–12. <https://doi.org/10.1007/s00430-013-0307-0>.
 30. Chabelskaya S, Gaillot O, Felden B. 2010. A *Staphylococcus aureus* small RNA is required for bacterial virulence and regulates the expression of an immune-evasion molecule. *PLoS Pathog* 6:e1000927. <https://doi.org/10.1371/journal.ppat.1000927>.
 31. Kaito C, Saito Y, Ikuo M, Omae Y, Mao H, Nagano G, Fujiyuki T, Numata S, Han X, Obata K, Hasegawa S, Yamaguchi H, Inokuchi K, Ito T, Hiramatsu K, Sekimizu K. 2013. Mobile genetic element SCCmec-encoded *psm-mec* RNA suppresses translation of *agrA* and attenuates MRSA virulence. *PLoS Pathog* 9:e1003269. <https://doi.org/10.1371/journal.ppat.1003269>.
 32. Kim S, Reyes D, Beaume M, Francois P, Cheung A. 2014. Contribution of teg49 small RNA in the upstream transcriptional region of *sarA* to virulence in *Staphylococcus aureus*. *Infect Immun* 82:4369–4379. <https://doi.org/10.1128/IAI.02002-14>.
 33. Fey FD, Endres JL, Yajjala VK, Widhelm TJ, Boissy RJ, Bose JL, Bayles KW. 2013. A genetic resource for rapid and comprehensive phenotype screening of nonessential *Staphylococcus aureus* genes. *mBio* 4:e00537-12. <https://doi.org/10.1128/mBio.00537-12>.
 34. Kim S, Corvaglia A-R, Leo S, Cheung A, Francois P. 2016. Characterization of RNA helicase CshA and its role in protecting mRNAs and small RNAs of *Staphylococcus aureus* strain Newman. *Infect Immun* 84:833–844. <https://doi.org/10.1128/IAI.01042-15>.
 35. Trotonda MP, Manna AC, Cheung AL, Lasa I, Penades JR. 2005. SarA control Bap-dependent biofilm formation in *Staphylococcus aureus*. *J Bacteriol* 187:5790–5798. <https://doi.org/10.1128/JB.187.16.5790-5798.2005>.
 36. Manna AC, Ingavale SS, Maloney M, van Wamel W, Cheung AL. 2004. Identification of *sarV* (SA2062), a new transcriptional regulator, is repressed by SarA and MgrA (SA0641) and involved in the regulation of autolysis in *Staphylococcus aureus*. *J Bacteriol* 186:5267–5280. <https://doi.org/10.1128/JB.186.16.5267-5280.2004>.
 37. Oun S, Redder P, Didier JP, Francois P, Corvaglia AR, Buttazzoni E, Giraud C, Girard M, Schrenzel J, Linder P. 2013. The CshA DEAD-box RNA helicase is important for quorum sensing control in *Staphylococcus aureus*. *RNA Biol* 10:157–165. <https://doi.org/10.4161/rna.22899>.
 38. Gottesman S, Storz S. 2011. Bacterial small RNA regulators: versatile roles and rapidly evolving variations. *Cold Spring Harb Perspect Biol* 3:a003798. <https://doi.org/10.1101/cshperspect.a003798>.
 39. Stead MB, Marshburn S, Mohanty BK, Mitra J, Pena Castillo L, Ray D, van Bakel H, Hughes TR, Kushner SR. 2011. Analysis of *Escherichia coli* RNase E and RNase III activity *in vivo* using tiling microarrays. *Nucleic Acids Res* 39:3188–3203. <https://doi.org/10.1093/nar/gkq1242>.
 40. Romilly C, Chevalier C, Marzi S, Masquida B, Geissmann T, Vandenesch F, Westhof E, Romby P. 2012. Loop-loop interactions involved in antisense regulation are processed by the endoribonuclease III in *Staphylococcus aureus*. *RNA Biol* 9:1461–1472. <https://doi.org/10.4161/rna.22710>.
 41. Geisinger E, Adhikari RP, Jin R, Ross HF, Novick RP. 2006. Inhibition of *rot* translation by RNAIII, a key feature of *agr* function. *Mol Microbiol* 61:1038–1048. <https://doi.org/10.1111/j.1365-2958.2006.05292.x>.
 42. Lioliou E, Sharma CM, Caldelari I, Hefer A-C, Fechter P, Vandenesch F, Romby P. 2012. Global regulatory functions of the *Staphylococcus aureus* endoribonuclease III in gene expression. *PLoS Genet* 8:e1002782. <https://doi.org/10.1371/journal.pgen.1002782>.
 43. Richards J, Liu Q, Pellegrini O, Celesnik H, Yao S, Bechhofer DH, Conon C, Belasco JG. 2011. An RNA pyrophosphohydrolase triggers 5'-exonucleolytic degradation of mRNA in *Bacillus subtilis*. *Mol Cell* 43:940–949. <https://doi.org/10.1016/j.molcel.2011.07.023>.
 44. Rowe SE, Campbell C, Lowry C, O'Donnell ST, Olson ME, Lindgren JK, Waters EM, Fey PD, O'Gara JP. 2016. AraC-type regulator Rbf controls the *Staphylococcus epidermidis* biofilm phenotype by negatively regulating the *icaADBC* repressor SarR. *J Bacteriol* 198:2914–2924. <https://doi.org/10.1128/JB.00374-16>.
 45. Gimpel M, Brantl S. 2017. Dual-function small regulatory RNAs in bacteria. *Mol Microbiol* 103:387–397. <https://doi.org/10.1111/mmi.13558>.
 46. Manna AC, Cheung AL. 2001. Characterization of *sarR*, a modulator of *sarA* expression in *Staphylococcus aureus*. *Infect Immun* 69:885–896. <https://doi.org/10.1128/IAI.69.2.885-896.2001>.
 47. Arnaud M, Chastanet A, Debarbouille M. 2004. New vector for efficient allelic replacement in naturally nontransformable, low-GC content Gram-positive bacteria. *Appl Environ Microbiol* 70:6887–6891. <https://doi.org/10.1128/AEM.70.11.6887-6891.2004>.
 48. O'Toole GA. 2011. Microtiter dish biofilm formation assay. *J Vis Exp* 41:2437. <https://doi.org/10.3791/2437>.
 49. Robinson MD, McCarthy DJ, Smyth GK. 2010. Edger: a bioconductor package for differential expression analysis of digital gene expression data. *Bioinformatics* 26:139–140. <https://doi.org/10.1093/bioinformatics/btp616>.
 50. Anders S, McCarthy DJ, Chen Y, Okoniewski M, Smyth GK, Huber W, Robinson MD. 2013. Count-based differential expression analysis of RNA sequencing data using R and Bioconductor. *Nat Protoc* 8:1765–1786. <https://doi.org/10.1038/nprot.2013.099>.
 51. Bunce C, Wheeler L, Reed G, Musser J, Barg N. 1992. Murine model of cutaneous infection with Gram-positive cocci. *Infect Immun* 60:2636–2640.
 52. Novick RP, Ross HF, Projan SJ, Kornblum J, Kreiswirth B, Moghazeh S. 1993. Synthesis of staphylococcal virulence factors is controlled by a regulatory RNA molecule. *EMBO J* 12:3967–3977.
 53. Horsburgh MJ, Clements MO, Crossley H, Ingham E, Foster SJ. 2002. σ^B modulates virulence determinants expression and stress resistance: characterization of a functional *rsbU* strain of *Staphylococcus aureus* 8325-4. *J Bacteriol* 184:5457–5467. <https://doi.org/10.1128/JB.184.19.5457-5467.2002>.